Title
DECAY INTO STRANGE BARYON-ANTIBARYON PAIRS and AW I-SPIN DETERMINATION OP THE (3095)

Author
Goldhaber, G.

Publication Date
1975-08-01

Talk presented at the IVth International
Nucleon-Antinucleon Symposium,
Syracuse, NY, May 2 - 4, 1975

LBL-4224
SLAC-PUB-1622

DECAY INTO STRANGE BARYON-ANTIBARYON PAIRS AND AN I-SPIN DETERMINATION OF THE $\psi(3095)$

G. Goldhaber, A. D. Johnson, J. A. Kadyk, W. Tanenbaum,
G. H. Trilling, G. S. Abrams, A. M. Boyarski, M. Breidenbach,
F. Bulos, W. Chinowsky, G. J. Feldman, C. E. Friedberg,
G. Hanson, D. L. Hartill, B. Jean-Marie, R. R. Larsen,
A. M. Litke, D. Lüke, B. A. Lulu, V. Lüth, H. L. Lynch,
C. C. Morehouse, J. M. Paterson, M. L. Perl, F. M. Pierre,
T. P. Pun, P. Rapidis, B. Richter, B. Sadoulet, R. F. Schwitters,
F. Vannucci, J. S. Whitaker, F. C. Winkelmann, and J. E. Wiss

August 15, 1975

Prepared for the U. S. Energy Research and
Development Administration under Contract W-7405-ENG-48

DISCLAIMER

Talk by G. Goldhaber at the IVth International Nucleon-Antinucleon Symposium, Syracuse University, Syracuse, NY, May 2-4, 1975

LBL-4224
SLAC-PUB-1622

DECAY INTO STRANGE BARYON-ANTIBARYON PAIRS AND AN I-SPIN DETERMINATION OF THE $\psi(3095)$*§

G. Goldhaber, A. D. Johnson, J. A. Kadyk, W. Tanenbaum, G. H. Trilling, G. S. Abrams, A. M. Boyarski, M. Breidenbach, F. Bulos, W. Chinowsky, G. J. Feldman, C. E. Friedberg, G. Hanson, D. L. Hartill†, B. Jean-Marie, R. R. Larsen, A. M. Litke, D. Lüke‡, B. A. Lulu, V. Lüth, H. L. Lynch, C. C. Morehouse, J. M. Paterson, M. L. Perl, F. M. Pierre††, T. P. Pun, P. Rapidis, B. Richter, B. Sadoulet, R. F. Schwitters, F. Vannucci‡‡, J. S. Whitaker, F. C. Winkelmann, and J. E. Wiss

Lawrence Berkeley Laboratory and Department of Physics
University of California, Berkeley, California 94720

Stanford Linear Accelerator Center
Stanford University, Stanford, California 94305

In our study of the decay modes of the $\psi(3095)$ the decay into baryon-antibaryon pairs stands out very clearly. While the branching ratio is small--a few tenths of one percent--the exclusive channels are readily identifiable. In this talk I will give the data for $\psi(3095)$ decay into $\Lambda\bar{\Lambda}$ and show some evidence for the channels $\Sigma\bar{\Sigma}$ and possibly $\Xi\bar{\Xi}$. The final states $\Sigma\bar{\Sigma}$ and $\Xi\bar{\Xi}$ are however ambiguous with $\Lambda\bar{\Lambda}X^{o}$; for example, $\Lambda\bar{\Lambda}\pi^{o}$.

The decay $$\psi(3095) \rightarrow \Lambda\bar{\Lambda} \qquad (1)$$ is of particular interest because the $\Lambda\bar{\Lambda}$ pair is in a pure I = 0 state. I will show that this decay proceeds <u>directly</u>, rather than through an intermediate γ, and thus obtain a determination of the I-spin of the $\psi(3095)$.

1. <u>$p\bar{p}$ Identification</u>

The present analysis is confined to events with two and four charged prongs observed in the SLAC-LBL Magnetic Detector at SPEAR. Experimental details have been presented earlier.[1] The protons and antiprotons are identified by

---

* Work supported by the U. S. Energy Research and Development Administration.

† Alfred P. Sloan Fellow.

‡ Fellow of Deutsche Forschungsgemeinschaft.

†† Centre d'Etudes Nucléaires de Saclay, Saclay, France.

‡‡ Institut de Physique Nucléaire, Orsay, France.

§ Data sample updated to August 15, 1975.

time-of-flight (TOF) measurements over a 1.5-meter minimum flight path combined with momentum measurements. The TOF resolution is ~ 0.5 nsec. At the $\psi(3095)$ the maximum possible proton momentum is 1231 MeV/c and a good separation of protons from other particles is achieved. The procedure followed here was to demand both a proton and antiproton pair in the final state. We estimate that the resulting sample of events of the types

$$\psi(3095) \rightarrow p\bar{p}\pi^+\pi^- \qquad (2)$$

and

$$\psi(3095) \rightarrow p\bar{p}\pi^+\pi^- + \text{neutral(s)} \qquad (3)$$

has a contamination of less than $\sim 10\%$. The data studied here consists of $\sim 50{,}000$ hadronic decays of $\psi(3095)$. Of these we identified 125 ± 12 events of reaction (2) and 91 ± 9 events of reaction (3). These events are shown in Fig. 1.

For branching ratio determinations we will compare the above events with the reaction

$$\psi(3095) \rightarrow p\bar{p} \qquad (4)$$

for which we have identified 105 ± 10 events in the same data sample.

Figure 2 shows a plot of the momentum of one track against that of the other track for all total charge-zero two-prong events. The large black spot centered at $P_1 = P_2 = 1547$ MeV/c represents the Bhabha scattering and μ-pair production events. The bands correspond to radiative Bhabha events. The enhancement at $P_1 = P_2 = 1231$ MeV/c corresponds to the $p\bar{p}$ pairs. Figure 3 shows the same distribution after the TOF $p\bar{p}$ identification is made. Figure 4 shows the effective mass distribution of all the identified two-prong $p\bar{p}$ pairs.

2. $\Lambda\bar{\Lambda}$ Identification

An examination of the $p\pi^-$ and $\bar{p}\pi^+$ mass spectrum shows striking Λ and $\bar{\Lambda}$ signals respectively. In Fig. 5 we show these masses plotted against each other and we find 43 clearly separated $\Lambda\bar{\Lambda}$ pairs. For these we estimate a contamination of less than 5%.

3. Kinematical Fitting[2]

We have modified the well-known bubble chamber fitting program, SQUAW, to accept and fit the events reconstructed from the SLAC-LBL Magnetic Detector. All events of types (2) and (3) were tried in the two-constraint fit

$$\psi(3095) \rightarrow \Lambda + \bar{\Lambda} + \text{MM} \qquad (5)$$

where MM stands for missing mass. This resulted in the same set of $\Lambda\bar{\Lambda}$ events shown in Fig. 5 but now with Λ and $\bar{\Lambda}$ momenta adjusted by the fit to give the more precisely known Λ and $\bar{\Lambda}$ masses.

Figure 6 gives a plot of these fitted momenta P_Λ versus $P_{\bar{\Lambda}}$. In Fig. 7 we show the angular deviation from collinearity in mrad plotted against the lower of the two Λ or $\bar{\Lambda}$ momenta.

It appears from these figures that the events tend to separate into three main categories. On the basis of kinematical fitting and testing with 0-constraint equations, the events can be associated with:

(A) $\psi(3095) \rightarrow \Lambda\bar{\Lambda}$ — 23 ± 5 events identified; final state $I = 0$

(B) $\psi(3095) \rightarrow \Sigma^0\bar{\Sigma}^0$, $\Sigma^0 \rightarrow \Lambda\gamma$, $\bar{\Sigma}^0 \rightarrow \bar{\Lambda}\gamma$ — 9 ± 3 events consistent with hypothesis; final state $I = 0$ or $I = 2$

(C) $\psi(3095) \rightarrow \Xi^0\bar{\Xi}^0$, $\Xi^0 \rightarrow \Lambda\pi^0$, $\bar{\Xi}^0 \rightarrow \bar{\Lambda}\pi^0$ — 3 ± 2 events consistent with hypothesis; final state $I = 0$ or $I = 1$

(D) $\psi(3095) \rightarrow \Lambda\bar{\Lambda}$ + neutral(s) — 8 events which cannot be assigned as above

It must be stressed however that the events in B and C are also consistent with $\psi(3095) \rightarrow \Lambda\bar{\Lambda}\pi^0$. Reaction A was fitted in the six-constraint sequence

$$\psi \rightarrow \Lambda\bar{\Lambda}, \quad \Lambda \rightarrow p\pi^-, \quad \bar{\Lambda} \rightarrow p\pi^+$$

and the events in the momentum region around 1073 MeV/c in Figs. 6 and 7 gave good χ^2 values for this hypothesis. The deviation from collinearity for these 23 ± 5 events is centered at 20 mrad with a maximum value of 50 mrad. We can place a limit on the reactions

(E) $\psi(3095) \rightarrow \Sigma^0\bar{\Lambda}$ or $\bar{\Sigma}^0\Lambda$

which are $I = 1$ in the final state. In Fig. 8 we show the missing mass squared distribution for each $\bar{\Lambda}$ against the same quantity for the Λ. Reaction A should be a point in this figure at $M^2_\Lambda = 1.243\ \text{GeV}^2$ in both variables. The size of the cluster around this region is a measure of the residual

error after fitting to the Λ and $\bar{\Lambda}$ masses. Reaction E will populate two lines at $M^2_{\Sigma^0} = 1.420$ GeV^2 on this plot uniformly (like on a Dalitz plot). These lines which extend from $M^2_{min} = 1.277$ GeV^2 to $M^2_{max} = 2.071$ GeV^2 are indicated on the figure. The lower ends of these lines extend into the region of reaction A. If we consider that over the upper 50% of these lines there is no population, then at the 90% confidence level we can say that there are at most 5 events corresponding to reaction E. This places an upper limit to the ratio $N(\Lambda\bar{\Sigma}^0 \text{ or } \bar{\Lambda}\Sigma^0)/N(\Lambda\bar{\Lambda}) \leq 5/23 = 22\%$. Reactions B and C are zero-constraint and thus no fit is possible. We have however ascertained that of the two remaining categories in Figs. 6 and 7, 9 ± 3 and 3 ± 2 events respectively are consistent with these hypotheses by solving the zero-constraint equations. However as stated $\psi(3095) \rightarrow \Lambda\bar{\Lambda}\pi^0$ cannot be excluded.

4. Efficiency Determination for $\Lambda\bar{\Lambda}$

To determine the actual $\Lambda\bar{\Lambda}$ branching ratio it is necessary to take account of the detection efficiency ϵ. This efficiency can be written as the product of two terms

$$\epsilon = \epsilon_G \, \epsilon_T$$

where ϵ_G is the geometrical efficiency, that is the probability that the event falls within the detector solid angle in which all tracks can be reconstructed, and ϵ_T is the probability that if the geometrical criteria are satisfied the event will generate an appropriate trigger, namely signals in at least two trigger counters and associated shower counters. We consider each in turn.

A. Trigger Efficiency

Normally with four particles within the solid angle subtended by the counters, the probability that at least two counters are fired is essentially unity. In the present situation this is slightly optimistic because (a) the pions are of relatively low momentum and hence have reduced efficiency for firing the shower counters, (b) the proton (but not the antiproton) can lose in the counters no more than its kinetic energy and hence also has less than unit efficiency in the lower part of its kinematically allowed momentum range. The actual efficiencies have been determined by studying the pattern of counter signals observed from each of the four particles for each $\Lambda\bar{\Lambda}$ event from which we find an average overall trigger efficiency of 0.93 ± 0.09.

B. Geometrical Efficiency

Charged particle tracks can be reconstructed with full

efficiency for angles greater than 53° (or less than 127°) relative to the beam. To make a simple efficiency calculation for Λ or $\bar{\Lambda}$, we note that the maximum proton angle relative to the Λ line of flight is 6.4°, and by confining ourselves therefore to Λ angles $\geq 53 + 6.4 = 59.4^\circ$, we guarantee that the p or $\bar{p}$ will be reconstructed. We then need only make a simple calculation for each detected $\Lambda\bar{\Lambda}$ event of the probability that the pions fall within the overall accepted solid angle, and derive therefrom an appropriate weight for the event. For the accepted events, the weights vary from 1.0 to 1.61. The total number of weighted events is 21.4 ± 6.6.

There is one other geometrical loss, namely Λ or $\bar{\Lambda}$ with very long flight paths. Studies of path length distributions indicate that there is a $7 \pm 3\%$ loss from long decay distance for each Λ or $\bar{\Lambda}$ and hence a $15 \pm 7\%$ correction to be applied overall. Figure 9 shows the Λ or $\bar{\Lambda}$ flight path distribution $c\tau$ in meters, converted to the Λ rest system. The quantity plotted (a) is the distance to the Λ vertex projected on to the Λ momentum $\vec{p}_\Lambda$ vs the mass of the $p\pi^-$ and $\bar{p}\pi^+$ systems. In (b) $c\tau$ is plotted for $\Lambda\bar{\Lambda}$ + (MM) events only.

Thus the total corrected number of

$$\begin{array}{l} \Lambda \quad \bar{\Lambda} \\ \big| \quad \big|\rightarrow \bar{p}\pi^+ \\ \big|\rightarrow p\pi^- \end{array}$$

events produced at $\geq 59.4^\circ$ to the beam axis is given by:

$$\frac{21.4 \pm 6.6}{0.93 \pm 0.09} (1.15 \pm 0.07) = 26.5 \pm 9.5 \quad .$$

Correcting for the $\Lambda \rightarrow p\pi^-$ branching ratio this becomes 64.3 ± 23.

Comparing now to the $p\bar{p}$ rate for purposes of obtaining a branching ratio, we observe 86 $p\bar{p}$ events in the same angular interval. Thus we find the ratio,

$$\frac{B_{\Lambda\bar{\Lambda}}}{B_{p\bar{p}}} = 0.75 \pm 0.27 \quad .$$

Using the directly determined value[3] for $B_{p\bar{p}} = 0.21 \pm 0.04\%$ we obtain $B_{\Lambda\bar{\Lambda}} = 0.16 \pm 0.07\%$.

5. An I-Spin Determination for $\psi(3095)$[4]

The final states $\Lambda\bar{\Lambda}$ is $I = 0$ while $\Sigma^0\bar{\Lambda}$ are $I = 1$. If the $\psi(3095)$ decays directly into the $\Lambda\bar{\Lambda}$ channel we have determined the I-spin to be zero. The argument we will use here

considers that

$$\psi(3095) \xrightarrow{\text{via } \gamma} \begin{matrix} \Lambda\bar{\Lambda} \\ \Sigma^{o}\bar{\Lambda} \\ \bar{\Sigma}^{o}\Lambda \end{matrix}$$

is in the ratio[5] 1 : 3 : 3 if the photon is a member of an SU(3) octet. Hence such a decay would demand six times as many $\Sigma^{o}\bar{\Lambda}$ and $\bar{\Sigma}^{o}\Lambda$ events combined as $\Lambda\bar{\Lambda}$ events. The experimental data given above clearly rules this possibility out. Hence we have determined that $I = 0$ for the $\psi(3095)$.

Alternately we can argue that since $B_{\Lambda\bar{\Lambda}}$ is comparable to $B_{p\bar{p}}$ the $\Lambda\bar{\Lambda}$ events are produced directly just as the $p\bar{p}$ events are. This argument can be sharpened by a study of $\Lambda\bar{\Lambda}$ production just below the $\psi(3095)$.

6. Discussion of the $\Sigma\bar{\Sigma}$ Hypothesis

There is a peculiarity associated with the 9 ± 3 events consistent with reaction B; i.e., $\psi(3095) \rightarrow \Sigma\bar{\Sigma}$, which is worth noting. On this assignment we would expect the events to uniformly populate the square labelled $\Sigma\bar{\Sigma}$ in Fig. 8. Instead the events appear to be concentrated above the diagonal connecting the upper lefthand and lower righthand corners. Aside from a statistical fluctuation we have no obvious explanation for such a distribution.

Kinematically the events also fall inside the Dalitz envelope for the reaction

(F) $\psi(3095) \rightarrow \Lambda\bar{\Lambda}\pi^{o}$

which is however $I = 1$ and thus inconsistent with the $I = 0$ determination for the $\psi(3095)$. An alternative possibility is

(G) $\psi(3095) \rightarrow \bar{\Lambda}\Sigma^{o}\pi^{o}$ and charge conjugate, which can be $I = 0$.

To resolve this ambiguity in a conclusive manner additional data will be required.

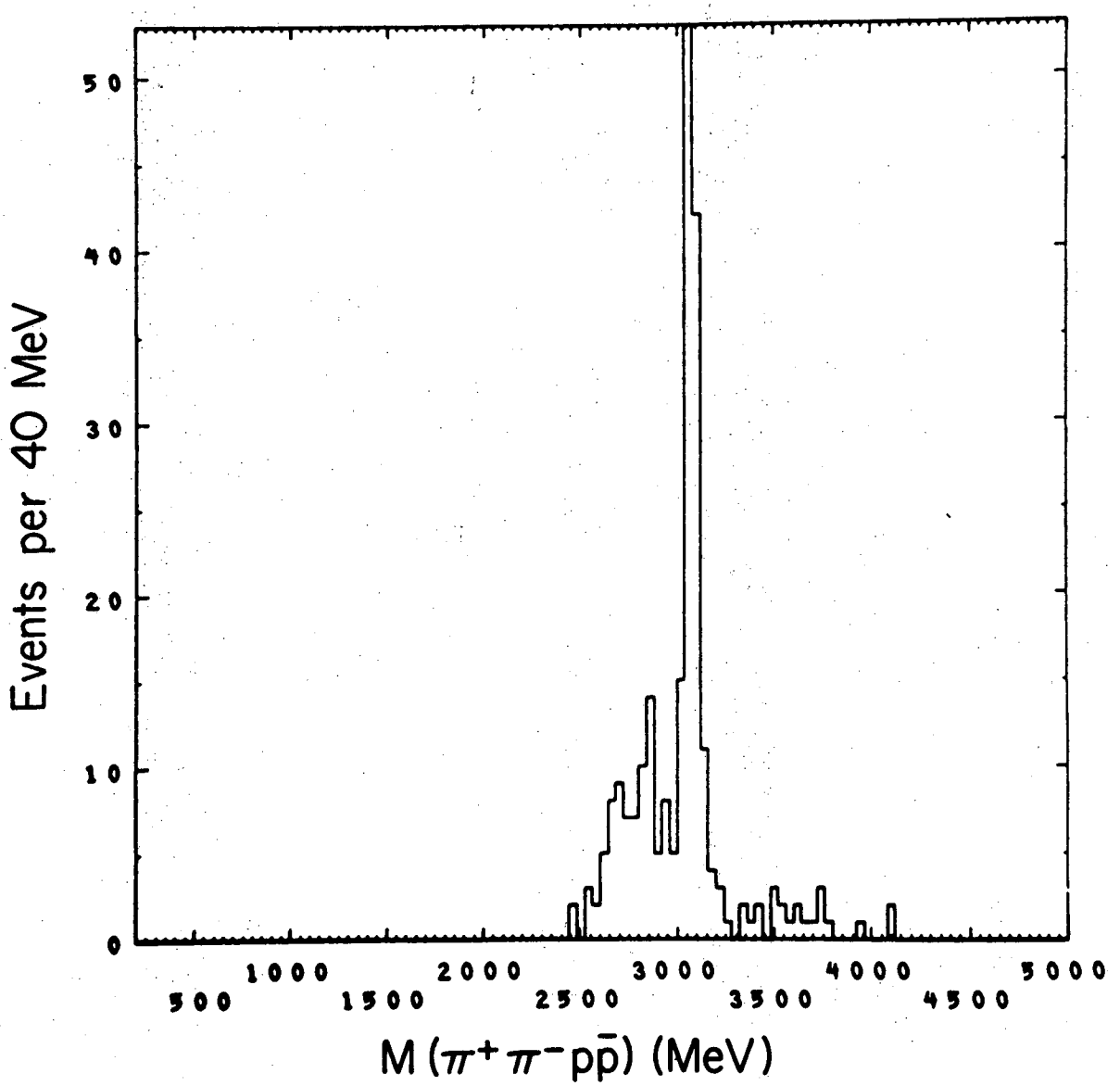

Fig. 1. The mass spectrum $M(\pi^+\pi^-p\bar{p})$ for the events with $p\bar{p}$ pairs "identified" by TOF and momentum. The peak corresponds to $\psi(3095) \rightarrow \pi^+\pi^-p\bar{p}$. The events below the peak have one or more neutral in addition. The events above the peak correspond to misidentified protons or antiprotons or to background events.

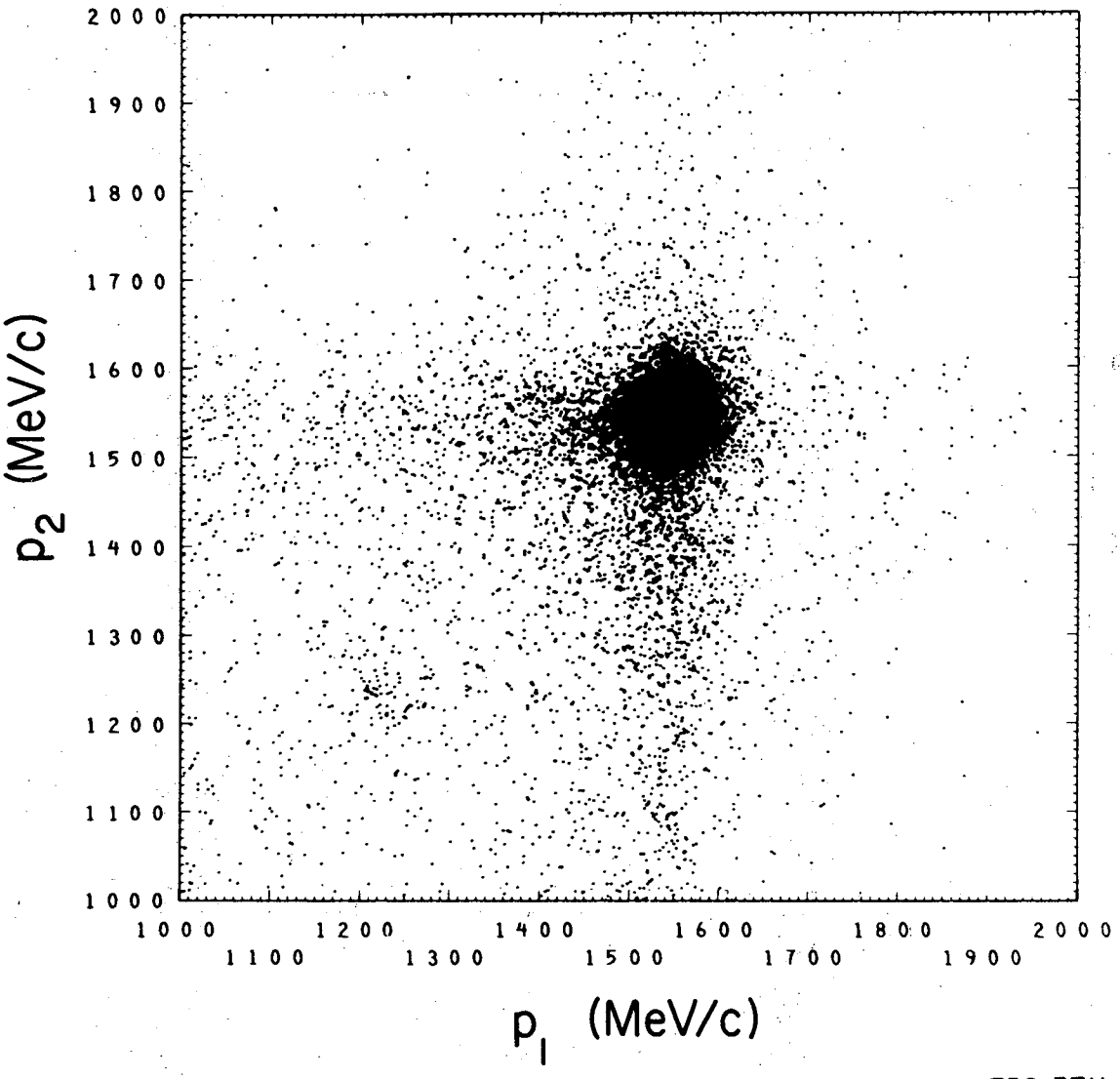

Fig. 2. Scatter plot of p_1 vs p_2 for events with 2 prongs, total charge zero. $\psi(3095) \rightarrow e^+e^-$, $\mu^+\mu^-$ and $p\bar{p}$.

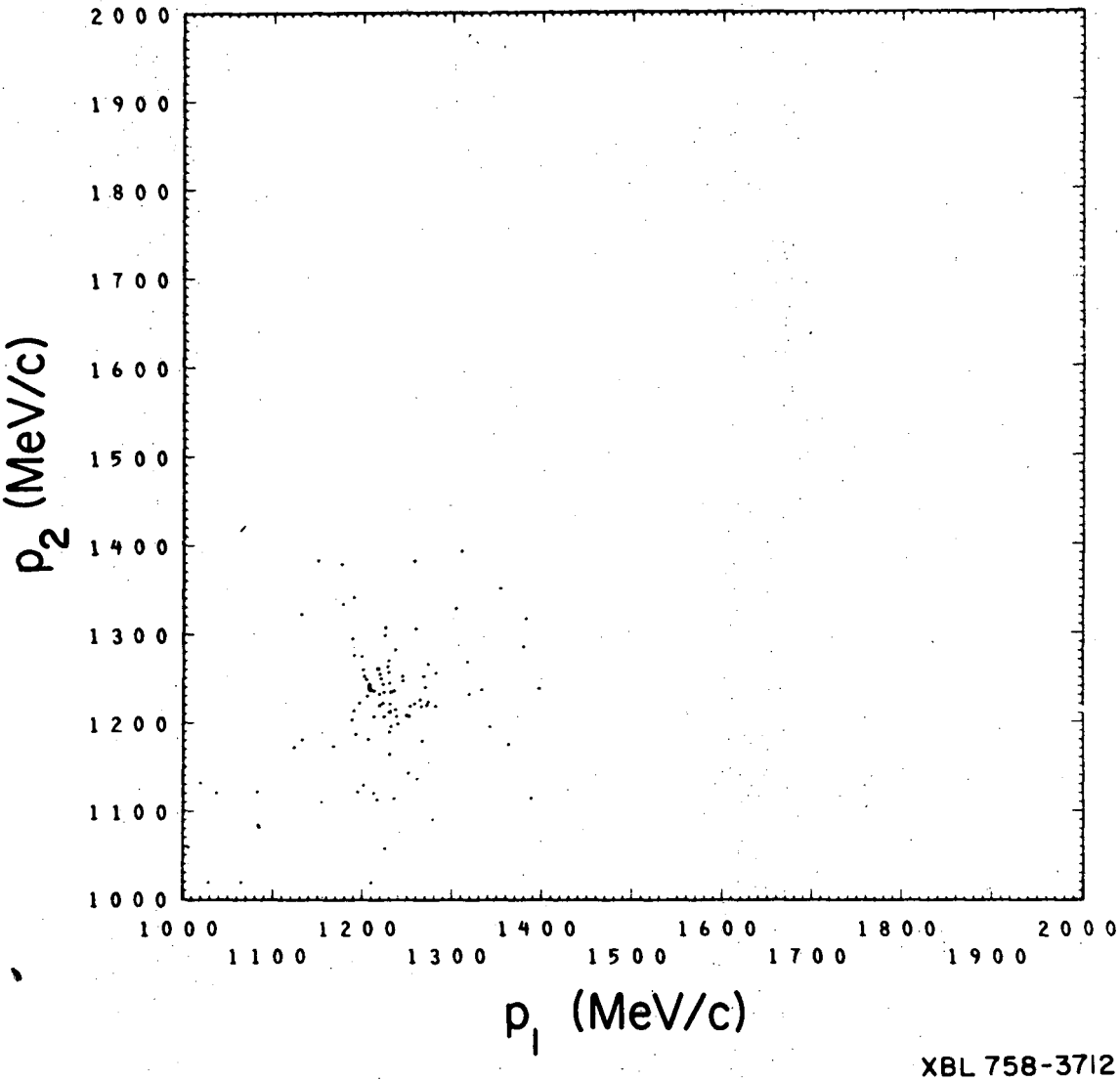

Fig. 3. Subset of scatter plot in Fig. 2 for $p\bar{p}$ pairs identified by TOF and momentum.

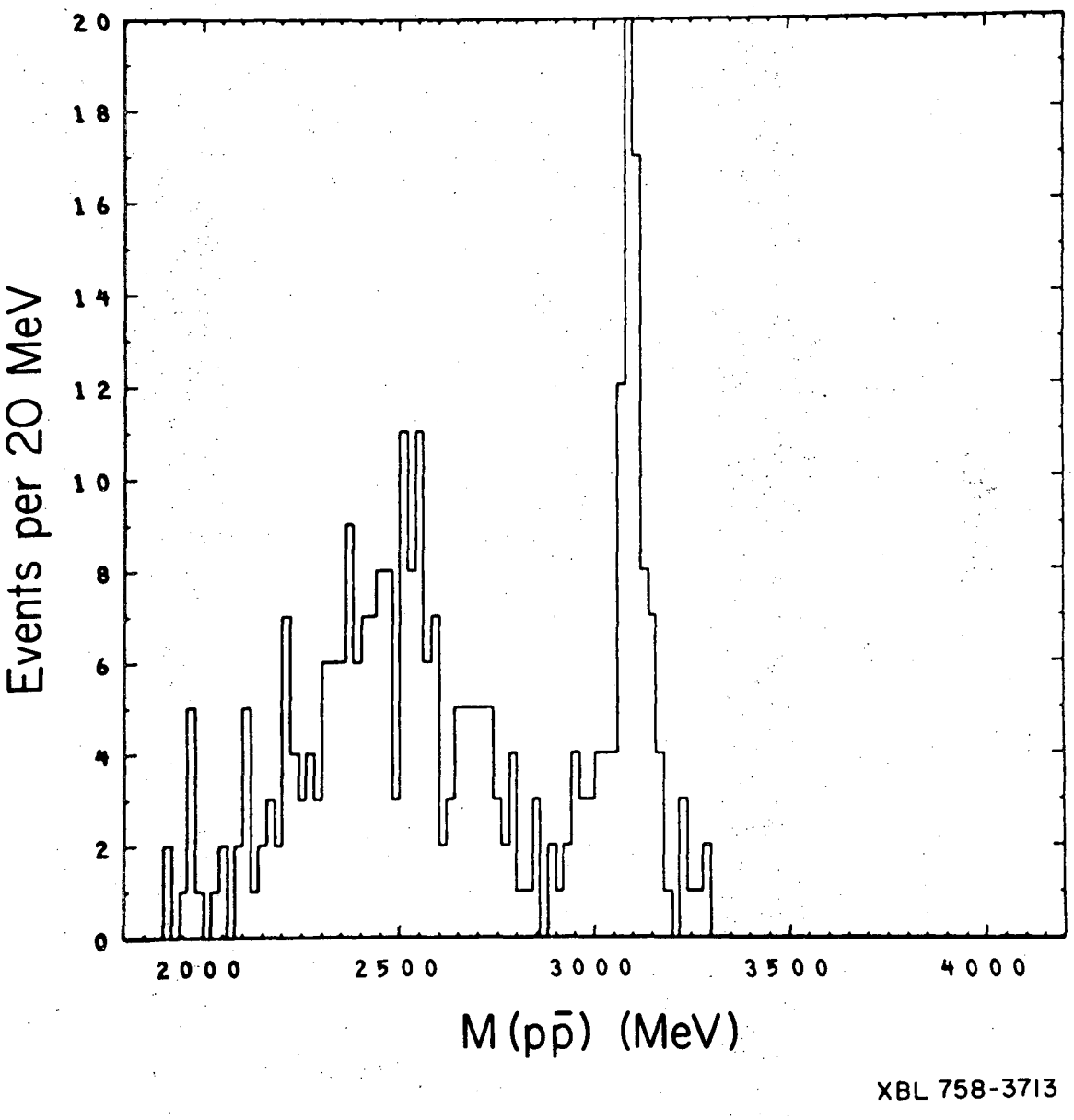

Fig. 4. Effective mass M($p\bar{p}$) for TOF identified $p\bar{p}$ pairs from 2-prong events.

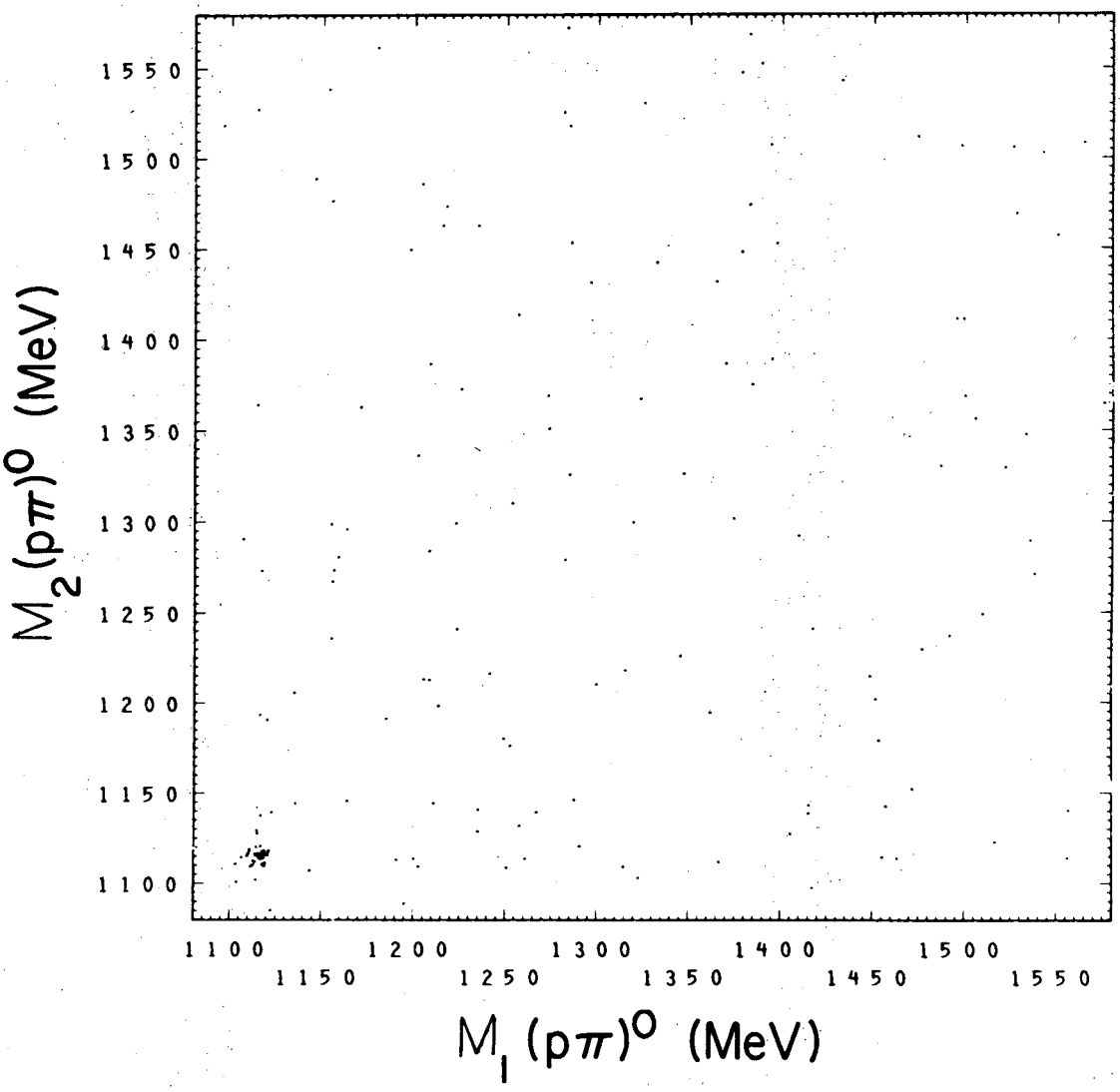

XBL 758-3714

Fig. 5. Scatter plot of $M_1(p\pi)^0$ vs $M_2(p\pi)^0$. This shows a clear $\Lambda\bar{\Lambda}$ signal with rather low background.

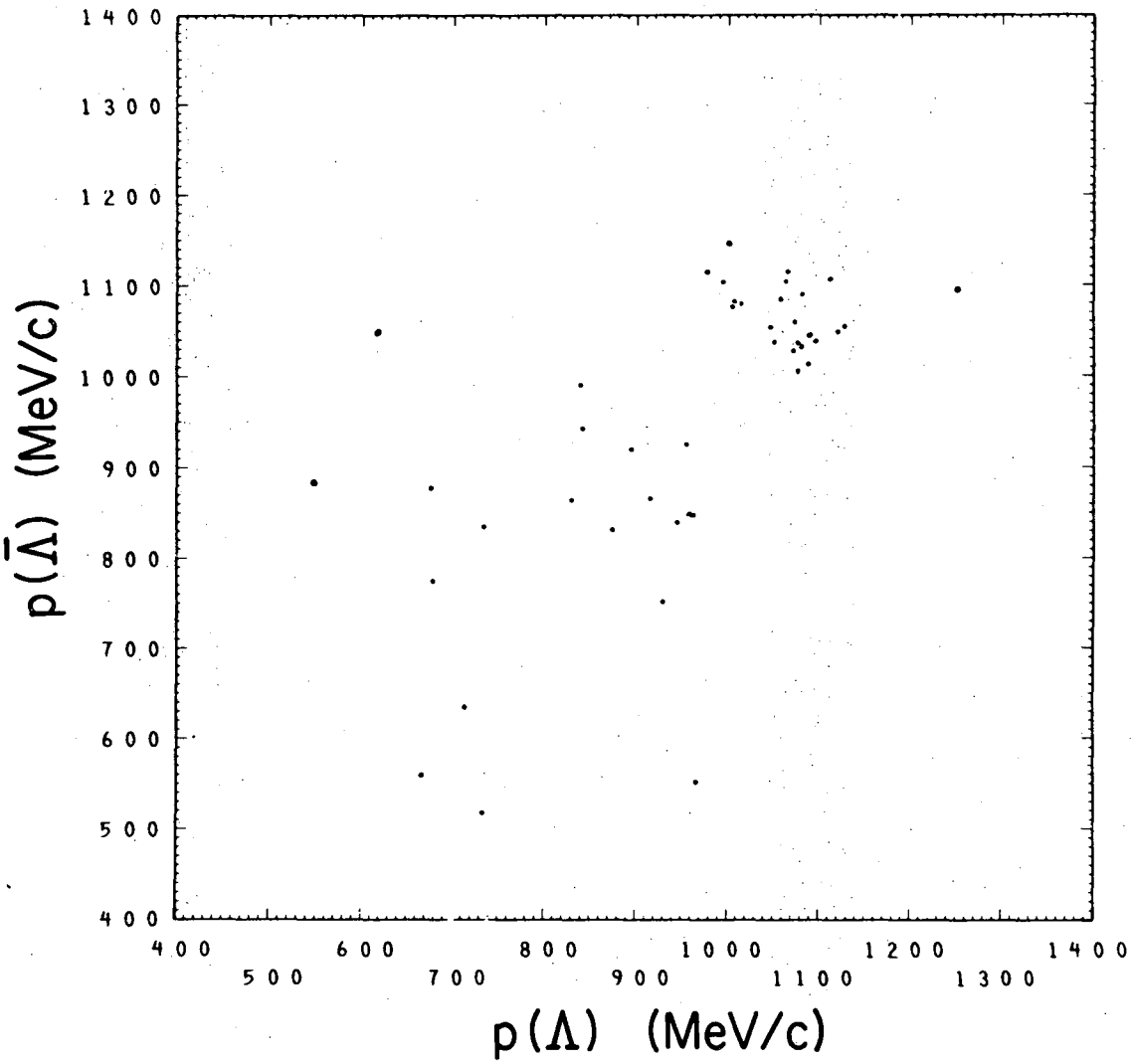

Fig. 6. $p_{\bar{\Lambda}}$ vs p_{Λ}.

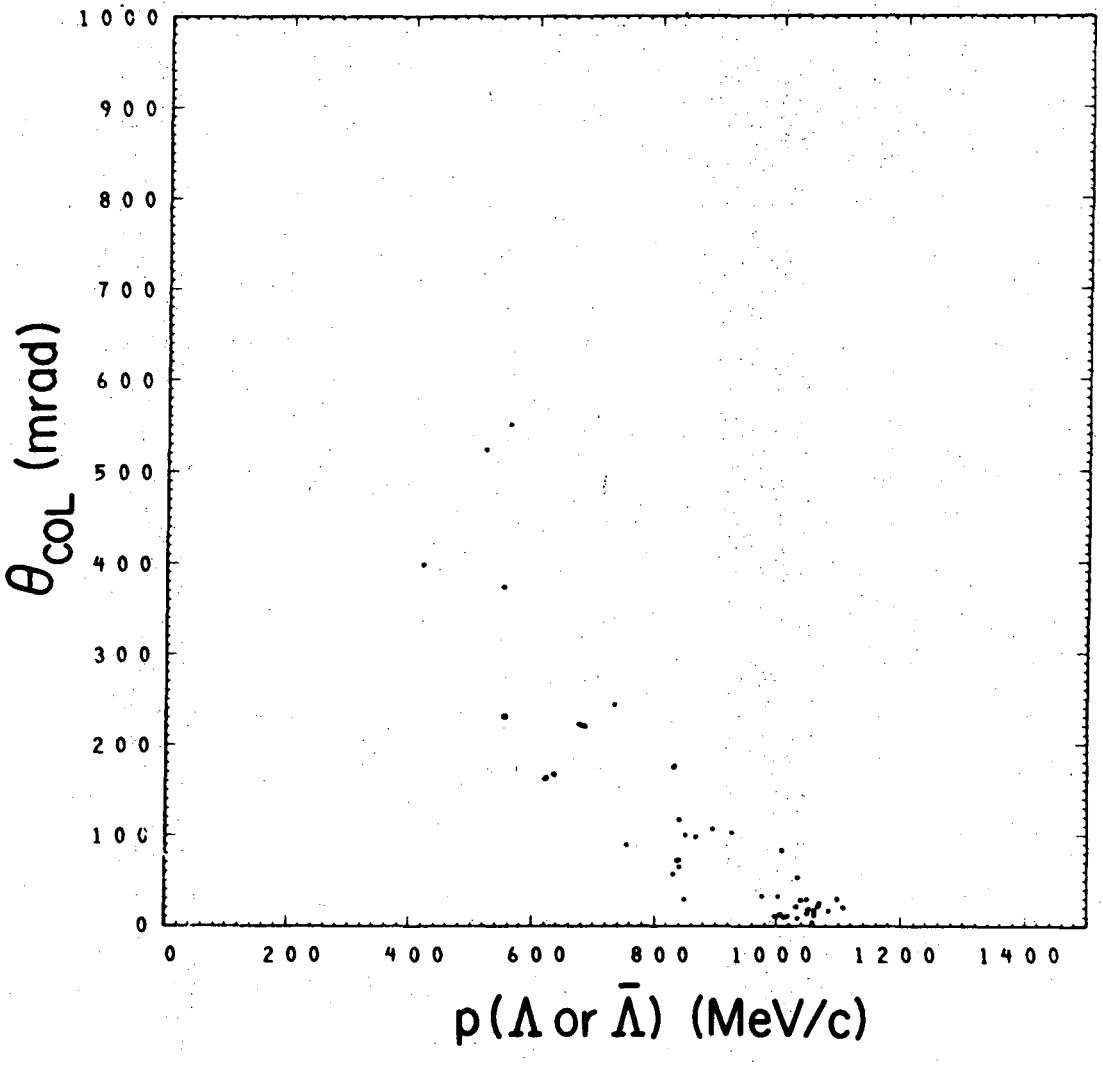

XBL 758-3716

Fig. 7. Angular deviation from collinearity vs the lower momenta of Λ or $\bar{\Lambda}$.

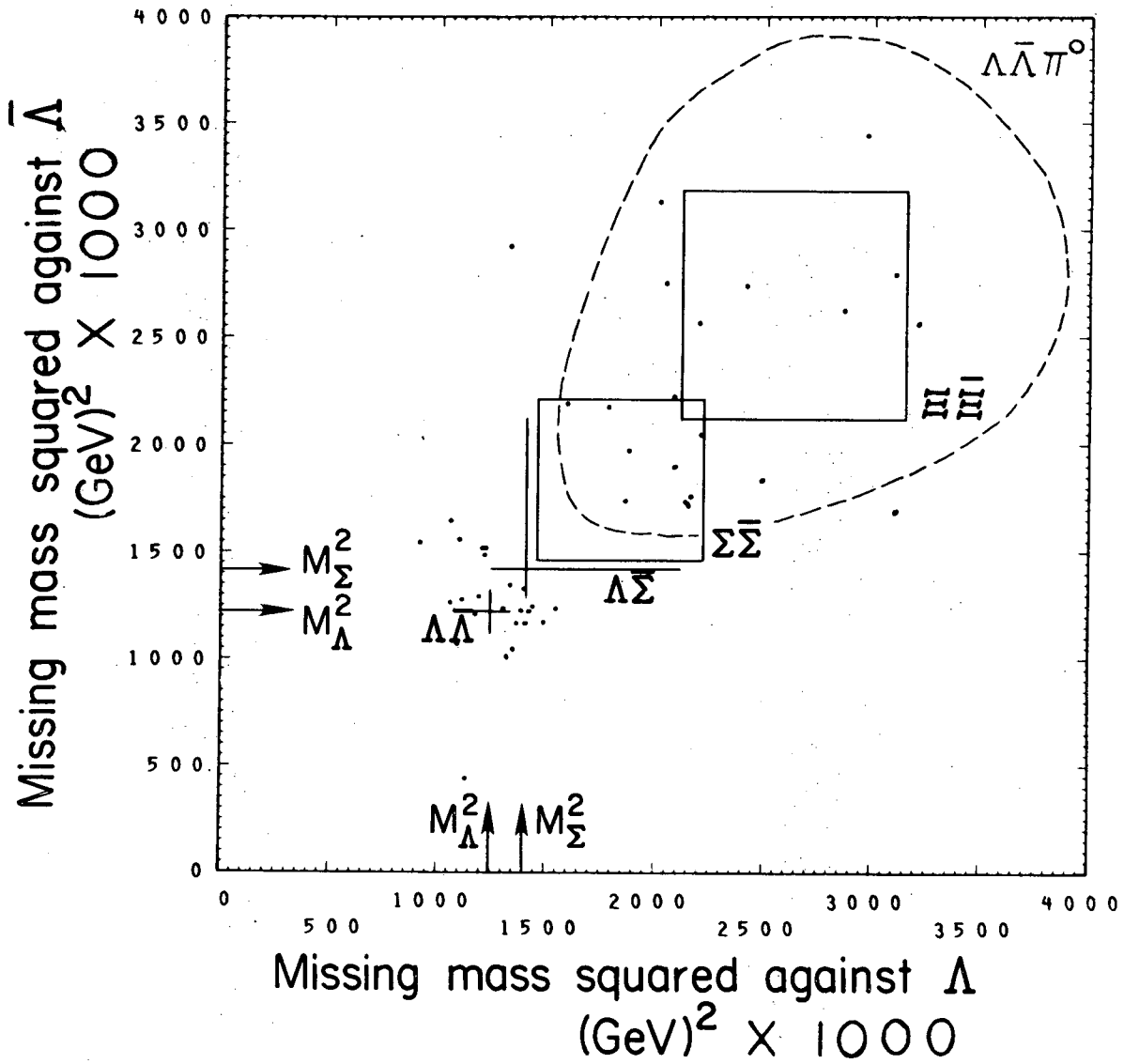

XBL 758-3717

Fig. 8. Missing mass squared against Λ vs that against $\bar{\Lambda}$. The regions corresponding to various final states are labelled on the figure. The dashed curve corresponds to the Dalitz envelope for the final state $\Lambda\bar{\Lambda}\pi^0$. As may be noted the events which fit the $\Sigma\bar{\Sigma}$ and $\Xi\bar{\Xi}$ hypotheses lie inside this curve and are thus ambiguous with this hypothesis.

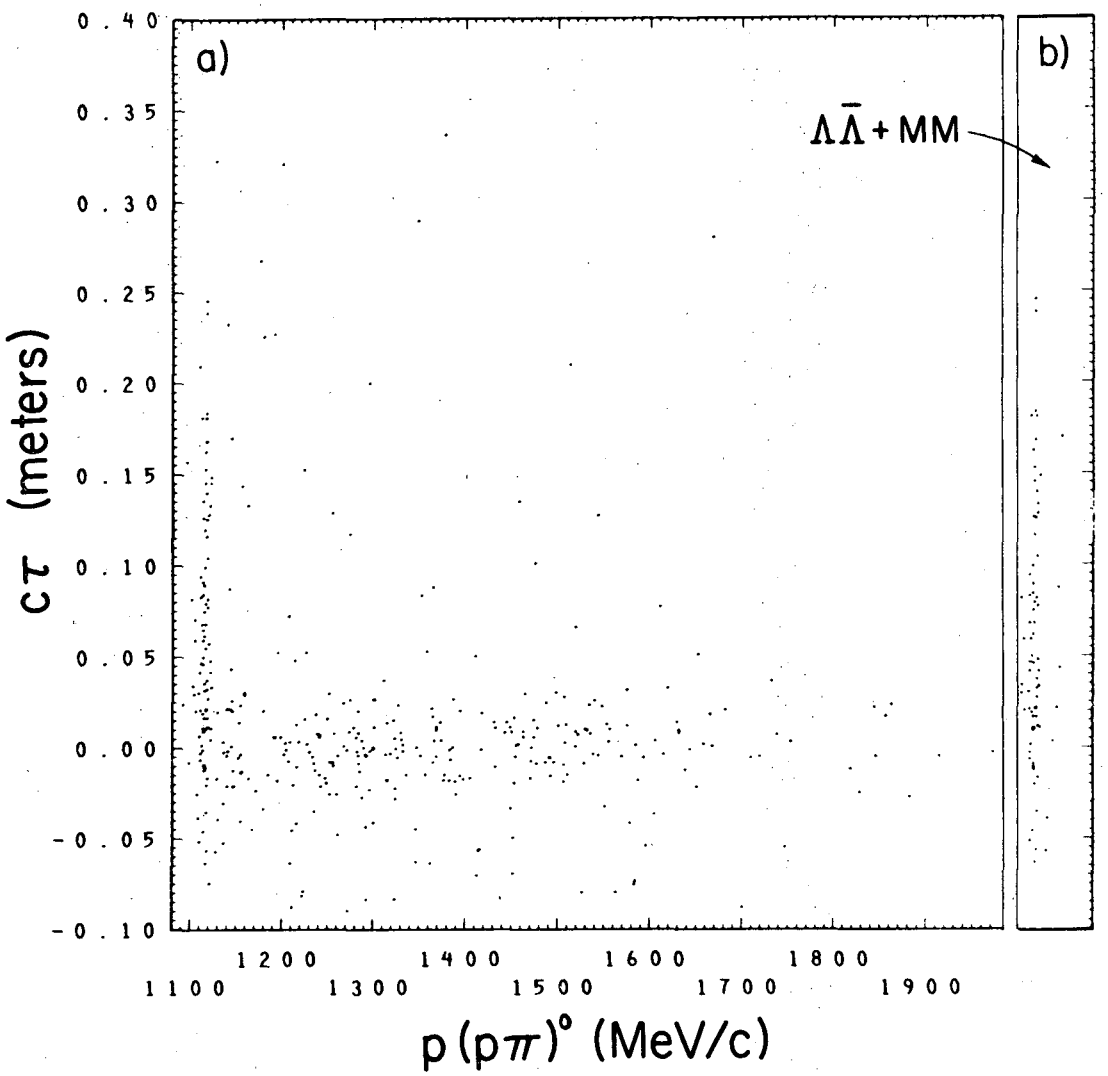

XBL 758-3718

Fig. 9. (a) cτ vs M(pπ)°. (b) cτ for $\Lambda\bar{\Lambda}$ + (MM) events. The known mean value for Λ decay is $c\tau_\Lambda$ = 0.077 meters.

References

1. J.-E. Augustin et al., Phys. Rev. Letters 34, 233 (1975).

2. We are grateful to Dr. O. Dahl of the Lawrence Berkeley Laboratory for help and consultations on the fitting programs.

3. A. M. Boyarski et al., Quantum Numbers and Decay Modes of the Resonances $\psi(3095)$ and $\psi(3684)$, SLAC-PUB-1599 and LBL-3897; talk presented at the International Conference for High Energy Physics, Palermo, Italy, 23-28 June 1975 by V. Lüth.

4. B. Jean-Marie et al. (to be published). This paper gives two other I-spin determinations; (a) from the decay $\psi(3095) \rightarrow \rho\pi$ which occurs equally for all charge combinations, (b) from $\psi(3095) \rightarrow p\bar{p}$, which is argued to proceed via strong interactions by the magnitude of the branching ratio, together with a determination of $G = -1$ from the decay mode $\psi(3095) \rightarrow 4\pi^{\pm}\pi^{o}$ and $C = -1$ from the production mechanism.

5. These conclusions were sharpened by discussions with F. Gilman of Stanford Linear Accelerator Center and M. Chanowitz of Lawrence Berkeley Laboratory.

TECHNICAL INFORMATION DIVISION
LAWRENCE BERKELEY LABORATORY
UNIVERSITY OF CALIFORNIA
BERKELEY, CALIFORNIA 94720